THERMAL POSTBUCKLING CHARACTERISTICS OF ANGLE-PLY LAMINATED TRUNCATED CIRCULAR CONICAL SHELLS

B.P. Patel*

Abstract

Here, the nonlinear thermoelastic pre- and post-buckling characteristics of angle-ply laminated composite conical shells subjected to uniform temperature rise are studied using semi-analytical finite element approach. The finite element formulation is based on first-order shear deformation theory and field consistency principle. The nonlinear governing equations, considering geometric nonlinearity based on von Karman's assumption for moderately large deformation, are solved using Newton-Raphson iteration procedure coupled with displacement control method to trace the prebuckling followed by postbuckling equilibrium path. The presence of asymmetric perturbation in the form of small magnitude load spatially proportional to the linear buckling mode shape is assumed to initiate the bifurcation of the shell deformation. The study is carried out to highlight the influences of semi-cone angle, ply-angles, number of layers and number of circumferential waves on the nonlinear prebuckling/postbuckling thermoelastic response of the laminated circular conical shells. The participation of axisymmetric and asymmetric modes in the total response of the shells is brought out through the deformation shape analysis.

Keywords : *Conical shell, Angle-ply, Thermal postbuckling, Critical temperature, Bifurcation, Semi-Analytical finite element, Nonlinear*

Introduction

The modern aeronautical and other engineering structures are often expected to operate at elevated temperatures. In this category belong the state of the art future transportation systems such as supersonic and hypersonic aircraft, rockets, satellites, as well as electronic equipment, nuclear components etc. The advances , in composite technology have lead to the application of elevated-temperature composite cylindrical/conical shells tailored for the required performance in the design of more and more sophisticated futuristic structures. The temperature rise in these structural components may introduce compressive membrane pre-stress state due to boundary restraints leading to thermoelastic buckling failures. An estimate of the critical buckling temperature can be made through a linear eigenvalue analysis, whereas the sensitivity to the imperfections and postbuckling behavior is evaluated by means of nonlinear analysis. For the later analysis, generally in the literature, an imperfection/perturbation affine to the critical buckling mode evaluated from eigenvalue analysis is assumed to be present in the shell structures.

The thermoelastic buckling analysis of composite laminated shells has received limited attention in the literature compared to that of isotropic shells and laminated panels [1-3]. The available studies on laminated shells are mostly dealing with the stability characteristics of circular cylindrical shells [4-17]. The stability characteristics of laminated composite cylindrical shells under thermal and mechanical loading situations are examined using Semiloof shell finite element [4, 5]. The improved Donnell's equations incorporating independent normal rotations are employed to study the thermal buckling of composite cylindrical shells under uniform temperature rise, radial and axial temperature differences [6]. The influence of piezoelectric actuators on the thermal buckling characteristics of laminated cylindrical shells [7] and thermal buckling of composite cylindrical shells conveying hot fluid [8] are examined using semi-analytical finite element based on first-order shear deformation theory. The critical buckling temperatures are estimated based on linear eigenvalue approach in Refs. [4-8].

The buckling and postbuckling response of composite shells subjected to high temperature is studied by Birman

* Department of Applied Mechanics, Indian Institute of Technology Delhi, Hauz Khas, New Delhi-110 016, India
Manuscript received on 24 Mar 2006; Paper reviewed and accepted on 17 Jan 2007

and Bert [9] employing nonlinear thermoelastic version of Love's first approximation theory and snap-through type of behavior is discussed qualitatively. The postbuckling analyses of perfect and imperfect, unstiffened and stiffened multi-layered cylindrical shells under thermo-mechanical loading situations have been performed using the von Karman-Donnell theory and employing singular perturbation approach [10-14]. The dynamic effects on the stability characteristics of laminated cylindrical shells arising due to the sudden application of the heat load [15, 16] and the presence of periodic time dependent temperature field [17] are also investigated in the literature.

The literature on the investigation of thermoelastic buckling characteristics of conical shells is scarce [18-24]. This may be attributed to the inherent complexity of the basic equations in curvilinear circular conical coordinates that are a system of nonlinear partial differential equations with variable coefficients. Bendavid and Singer [18] studied buckling of truncated isotropic conical shells heated along an axial strip using Rayleigh-Ritz method whereas Lu and Chang [19] and Chang and Lu [20] examined the thermoelastic buckling based on linear [19] and nonlinear [20] analyses employing Galerkin's method. The effects of the axisymmetric initial deflection [21] and internal pressure [22] are examined by Tani on the thermal buckling of shallow, truncated isotropic conical shells under uniform heating. The Donnel-type shell equations with nonlinear prebuckling deflections are solved using a semi-analytical finite difference method [21, 22]. Thermoelastic buckling [23] and thermally induced dynamic instability [24] of laminated composite conical shells are investigated employing perturbation approach to solve the linear three-dimensional equations of motion in terms of incremental stresses perturbed from the state of neutral equilibrium. The initial prebuckling thermal stresses are evaluated directly by multiplying thermal strains (product of thermal expansion coefficients and temperature rise) with constitutive matrix in Refs. [23, 24]. However, it has been brought out in the literature that the prebuckling state of stress has to be determined using the deformation field obtained from the static analysis of the shells subjected to assumed thermal load distribution.

In order to fully exploit the strength and load carrying capacity of laminated composite conical shells at elevated temperatures, accurate prediction of their thermal buckling/postbuckling characteristics is essential. However, to the best of author's knowledge, the study on the thermoelastic buckling/postbuckling behavior of laminated conical shells based nonlinear analysis appears to be scarce in the literature. The participation of axisymmetric/asymmetric modes is also not brought out in the limited number of analytical investigations available on thermal postbuckling behavior of laminated cylindrical shells. Furthermore, the available studies on thermal postbuckling of laminated cylindrical shells are confined to cross-ply lamination schemes.

Therefore, in the present work, the thermoelastic buckling/postbuckling characteristics of angle-ply truncated circular conical/cylindrical shells subjected to uniform temperature rise are studied through nonlinear static analysis employing semi-analytical finite element approach. The presence of asymmetric perturbation in the form of small magnitude load spatially proportional to the linear buckling mode shape is assumed to initiate the bifurcation of the shell deformation from axisymmetric mode to asymmetric one. The study is carried out to highlight the influences of semi-cone angle, ply-angles, number of layers and number of circumferential waves on the nonlinear prebuckling/postbuckling thermoelastic response of the laminated circular conical shells. The participation of axisymmetric and asymmetric modes in the total response of the shells is brought out through the deformation shape analysis.

Formulation

An axisymmetric laminated composite shell of revolution is considered with the coordinates s, θ and z along the meridional, circumferential and radial/thickness directions, respectively. The displacements u, v, w at a point (s, θ, z) from the median surface are expressed as functions of middle-surface displacements u_o, v_o and w_o , and independent rotations β_s and β_θ of the meridional and hoop sections, respectively, as

$$u(s, \theta, z) = u_o(s, \theta) + z\,\beta_s(s, \theta)$$
$$v(s, \theta, z) = v_o(s, \theta) + z\,\beta_\theta(s, \theta)$$
$$w(s, \theta, z) = w_o(s, \theta) \qquad (1)$$

Using the semi-analytical approach, u_o, v_o, w_o, β_s and β_θ are represented by a Fourier series in the circumferential angle θ. For the n^{th} harmonic, these can be written as

$$u_s(s, \theta) = u_o^o(s) + \sum_{i=1}^{4} \left[u_o^{c_i}(s) \cos(in\theta) + u_o^{s_i}(s) \sin(in\theta) \right]$$

$$v_o(s,\theta) = v_o^o(s) + \sum_{i=1}^{4}\left[v_o^{c_i}(s)\cos(in\,\theta) + v_o^{s_i}(s)\sin(in\,\theta)\right]$$

$$w_o(s,\theta) = w_o^o(s) + \sum_{i=1}^{2}\left[w_o^{c_i}(s)\cos(in\,\theta) + w_o^{s_i}(s)\sin(in\,\theta)\right]$$

$$\beta_s(s,\theta) = \beta_s^o(s) + \sum_{i=1}^{2}\left[\beta_s^{c_i}(s)\cos(in\,\theta) + \beta_s^{s_i}(s)\sin(in\,\theta)\right]$$

$$\beta_\theta(s,\theta) = \beta_\theta^o(s) + \sum_{i=1}^{2}\left[\beta_\theta^{c_i}(s)\cos(in\,\theta) + \beta_\theta^{s_i}(s)\sin(in\,\theta)\right] \tag{2}$$

where superscript *o* refers to the axisymmetric component of displacement field variables, and c_i and s_i refer to the asymmetric components of the field variables having circumferential variation proportional to cos (*in*θ) and sin (*in*θ), respectively.

The above displacement variations in the circumferential direction are chosen according to the physics of the large deformation of shells of revolution i. e. participation of axisymmetric mode and higher asymmetric modes [25-28]. Additional terms in the in-plane displacements, compared to radial displacement, are added to keep the nonlinear membrane strains consistent.

Using von Karman's assumption for moderately large deformation, Green's strains can be written in terms of mid-plane deformations as,

$$\{\varepsilon\} = \begin{Bmatrix} \varepsilon_p^L \\ 0 \end{Bmatrix} + \begin{Bmatrix} z\varepsilon_b \\ \varepsilon_s \end{Bmatrix} + \begin{Bmatrix} \varepsilon_p^{NL} \\ 0 \end{Bmatrix} \tag{3}$$

where, the membrane strains $\left\{\varepsilon_p^L\right\}$, bending strains $\{\varepsilon_b\}$, shear strains $\{\varepsilon_s\}$ and nonlinear in-plane strains $\left\{\varepsilon_p^{NL}\right\}$ in the equation (3) are written as [29]

$$\left\{\varepsilon_p^L\right\} = \begin{Bmatrix} \dfrac{\partial u_o}{\partial s} + \dfrac{w_o}{R} \\ \dfrac{u_o \sin\phi}{r} + \dfrac{\partial v_o}{r\partial\theta} + \dfrac{w_o\cos\phi}{r} \\ \dfrac{\partial u_o}{r\partial\theta} - \dfrac{v_o\sin\phi}{r} + \dfrac{\partial v_o}{\partial s} \end{Bmatrix};$$

$$\{\varepsilon_b\} = \begin{Bmatrix} \dfrac{\partial \beta_s}{\partial s} \\ \dfrac{\beta_s \sin\phi}{r} + \dfrac{\partial \beta_\theta}{r\partial\theta} \\ \dfrac{\partial \beta_s}{r\partial\theta} + \dfrac{\partial \beta_\theta}{\partial s} - \dfrac{\beta_\theta \sin\phi}{r} \end{Bmatrix};$$

$$\{\varepsilon_s\} = \begin{Bmatrix} \beta_s + \dfrac{\partial w_o}{\partial s} \\ \beta_\theta + \dfrac{\partial w_o}{r\partial\theta} - \dfrac{v_o\cos\phi}{r} \end{Bmatrix};$$

$$\left\{\varepsilon_p^{NL}\right\} = \begin{Bmatrix} \dfrac{1}{2}\left(\dfrac{\partial w_o}{\partial s}\right)^2 \\ \dfrac{1}{2}\left(\dfrac{\partial w_o}{r\partial\theta}\right)^2 \\ \dfrac{\partial w_o}{\partial s}\dfrac{\partial w_o}{r\partial\theta} \end{Bmatrix}; \tag{4}$$

where *r*, *R* and ϕ are the radius of the parallel circle, radius of the meridional circle and angle made by the tangent at any point in the shell with the axis of revolution.

If {***N***} represents the stress resultants (N_{ss}, $N_{\theta\theta}$, $N_{s\theta}$) and {***M***} the moment resultants (M_{ss}, $M_{\theta\theta}$, $M_{s\theta}$), one can relate these to membrane strains $\{\varepsilon_p\}$ $\left(=\left\{\varepsilon_o^L\right\} + \left\{\varepsilon_o^{NL}\right\}\right)$ and bending strains $\{\varepsilon_b\}$ through the constitutive relations as

$$\begin{Bmatrix} \{N\} \\ \{M\} \end{Bmatrix} = \begin{bmatrix} [A] & [B] \\ [B] & [D] \end{bmatrix} \begin{Bmatrix} \{\varepsilon_p\} \\ \{\varepsilon_b\} \end{Bmatrix} - \begin{Bmatrix} \{\bar{N}\} \\ \{\bar{M}\} \end{Bmatrix} \tag{5}$$

where [A], [D] and [B] are extensional, bending and bending-extensional coupling stiffness coefficients matrices of the composite laminate. $\{\bar{N}\}$ and $\{\bar{M}\}$ are the thermal stress and moment resultants, respectively.

Similarly, the transverse shear force $\{Q\}$ representing the quantities $(Q_{sz}, Q_{\theta z})$ are related to the transverse shear strains $\{\varepsilon_s\}$ through the constitutive relation as

$$\{Q\} = [E]\{\varepsilon_s\} \tag{6}$$

where [E] is the transverse shear stiffness coefficients matrix of the laminate.

For a laminated shell of thickness h, consisting of N layers with stacking angles θ_i ($i = 1, \ldots, N$) and layer thicknesses h_i ($i = 1, \ldots, N$), the necessary expressions to compute the stiffness coefficients and thermal stress/moment resultants, available in the literature [30] are used here.

The potential energy functional $U_1(\delta)$ (due to strain energy and transverse load) is given by,

$$U_1(\delta) = \frac{1}{2}\int_A \begin{Bmatrix} \varepsilon_p \\ \varepsilon_b \end{Bmatrix}^T \begin{bmatrix} A & B \\ B & D \end{bmatrix} \begin{Bmatrix} \varepsilon_p \\ \varepsilon_b \end{Bmatrix} + \{\varepsilon_s\}^T [E] \{\varepsilon_s\} - \begin{bmatrix} \begin{Bmatrix} \varepsilon_p \\ \varepsilon_b \end{Bmatrix}^T \begin{Bmatrix} \bar{N} \\ \bar{M} \end{Bmatrix} \end{bmatrix} dA - \int_A q w_o \, dA \tag{7}$$

where δ is the vector of degrees of freedom associated to the displacement field in a finite element discretisation and q is the applied external pressure load.

The potential energy $U_2(\delta)$ due to initial state of in-plane stress resultants $\{N^0\} = \{N^0_{ss}\ N^0_{\theta\theta}\ N^0_{s\theta}\}$ is written as

$$U_2(\delta) = \int_A \{\varepsilon_{NL}\}^T \{N^0\}\, dA \tag{8}$$

Following the procedure given in the work of Rajasekaran and Murray [31], the total potential energy functional $U(\delta)$ [$= U_1(\delta) + U_2(\delta)$] can be expressed as

$$U(\delta) = \{\delta\}^T [(1/2)[[K] - [K_T] + [K_G]] + (1/6)[N_1(\delta)] + (1/12)[N_2(\delta)]]\{\delta\} - \{\delta\}^T \{F_M\} - \{\delta\}^T \{F_T\} \tag{9}$$

where [K] is the linear stiffness matrix, [N_1] and [$N2$] are nonlinear stiffness matrices linearly and quadratically dependent on the field variables, respectively. [K_T] and [K_G] are the geometric stiffness matrices due to thermal and initial stress resultants. $\{F_M\}$ and $\{F_T\}$ are mechanical and thermal load vectors.

The minimization of total potential $U(\delta)$ given in equation (9) with respect to vector of degrees of freedom δ leads to the governing equation for the deformation of the shell as

$$[[K] - [K_T] + [K_G] + (1/2)[N_1(\delta)] + (1/3)[N_2(\delta)]]\{\delta\} = \{F_M\} + \{F_T\} \tag{10}$$

The governing equation (10) can be employed to study the linear/nonlinear static and eigenvalue buckling analyses by neglecting the appropriate terms as:

Linear Static Analysis :

$$[K]\{\delta\} = \{F_M\} + \{F_T\} \tag{11}$$

Nonlinear Static Analysis

$$[[K] - [K_T] + (1/2)[N_1(\delta)] + (1/3)[N_2(\delta)]]\{\delta\} = \{F_M\} + \{F_T\} \tag{12}$$

Eigenvalue Buckling Analysis :

$$[K]\{\delta\} = \Delta T \left[K^*_G\right]\{\delta\} \tag{13}$$

where $\left[\boldsymbol{K}_G^*\right]$ is the geometric stiffness due initial state of stress developed because of unit uniform temperature rise and ΔT is the temperature rise.

It may be noted here that for the purpose of evaluating $\left[\boldsymbol{K}_G^*\right]$, firstly the static analysis of the shell using equation (11) for unit temperature rise is carried out. The resulting deformation filed is used to calculate the initial state of stress resultants using equation (5) and in turn, for evaluating the $\left[\boldsymbol{K}_G^*\right]$ matrix.

The nonlinear prebuckling followed by postbuckling equilibrium path is traced by solving equation (12) using Newton-Raphson iteration procedure coupled with displacement control method [32]. The equilibrium is achieved for each load/displacement step until the convergence criteria suggested by Bergan and Clough [33] are satisfied within the specific tolerance limit of less than one percent.

Element Description

The laminated axisymmetric shell element used here is a C^0 continuous shear flexible element and has 33 nodal degrees of freedom

$$(u_o^o, u_o^{c1}, u_o^{s1}, u_o^{c2}, u_o^{s2}, u_o^{c3}, u_o^{s3}, u_o^{c4}, u_o^{s4},$$

$$v_o^o, v_o^{c1}, v_o^{s1}, v_o^{c2}, v_o^{s2}, v_o^{c3}, v_o^{s3}, v_o^{c4}, v_o^{s4},$$

$$w_o^o, w_o^{c1}, w_o^{s1}, w_o^{c2}, w_o^{s2},$$

$$\beta_s^o, \beta_s^{c1}, \beta_s^{s1}, \beta_s^{c2}, \beta_s^{s2}, \beta_\theta^o, \beta_\theta^{c1}, \beta_\theta^{s1}, \beta_\theta^{c2}, \beta_\theta^{s2})$$

at the three nodes in a curved element leading to 99 degrees of freedom per element.

If the interpolation functions for three-noded element are used directly to interpolate the five field variables u_o, v_o, w_o, β_s and β_θ in deriving the transverse shear and membrane strains, the element will lock and show oscillations in the shear and membrane stresses. Field consistency requires that the membrane and transverse shear strains must be interpolated in a consistent manner. Thus, β_s term in the expression for $\{\varepsilon_s\}$ given in equation (4) has to be consistent with the field function $\partial w_o/\partial s$ as shown in the works of Balakrishna and Sarma [34] and Prathap and Ramesh Babu [35]. Similarly the w_o and (u_o, v_o) terms in the expression of $\left\{\begin{matrix}L\\ \varepsilon\\ p\end{matrix}\right\}$ (first and third strain components) have to be consistent with the field functions $\partial u_o/\partial s$ and $\partial v_o/\partial s$, respectively. This is achieved by using the field redistributed substitute shape functions to interpolate those specific terms that must be consistent as described by Prathap and Ramesh Babu [35]. The element derived in this fashion behaves very well for both thick and thin situations, and permits the greater flexibility in the choice of integration order for the energy terms. Since the element is based on the field consistency approach, all the strain energy terms are evaluated using exact numerical integration scheme with respect to the meridional coordinate (s). The integration in the circumferential direction is carried out explicitly. The element developed here has good convergence and has no spurious rigid modes.

Results and Discussions

Here, the thermoelastic nonlinear prebuckling path followed by postbuckling characteristics of laminated truncated circular conical shells ($1/R$=0) subjected to uniform temperature rise are investigated using the semi-analytical finite element formulation described above. The radius of the parallel circle for the circular conical shell is described as $r = r_1 + (r_2\text{-}r_1)\, s/L$ where r_1 and r_2 are the parallel circular radii at the small and large end of the conical shell, and L is the slant length. The study is carried out to highlight the influences of semi-cone angle (ϕ), ply-angle (θ), number of layers (N) and number of circumferential waves (n) on the nonlinear prebuckling/postbuckling response in the form of relationship between maximum outward normal displacement parameter (w_{max}/h) versus temperature parameter T ($= \Delta T\, \alpha_L\, r_1/h$) for the laminated circular conical shells.

The material properties used, unless otherwise specified, are

$$E_L = 172.25\ GPa,\ E_T = 6.89\ GPa,\ G_{LT} = 3.445\ GPa,$$

$$G_{TT} = 1.378\ GPa,\ \nu_{LT} = \nu_{TT} = 0.25,$$

$$\alpha_L = 6.3 \times 10^{-6}/^0C,\ \alpha_T = 3\ \alpha_L$$

where *E, G, v* and α are Young's modulus, shear modulus, Poisson's ratio and coefficient of thermal expansion, respectively. Subscripts L and T are the longitudinal and transverse directions respectively with respect to the fibers. All the layers are of equal thickness and the ply-angle is measured with respect to the meridional axis (*s*-axis). The first layer is the innermost layer of the shell.

The details of simply supported and clamped-clamped immovable boundary conditions of the shells considered here are:

Simply supported:

$$u_o^o = u_o^{c1} = u_o^{s1} = u_o^{c2} = u_o^{s2} = u_o^{c3} = u_o^{s3} = u_o^{c4} = u_o^{s4}$$

$$= v_o^o = v_o^{c1} = v_o^{s1} = v_o^{c2} = v_o^{s2} = v_o^{c3} = v_o^{s3} = v_o^{c4} = v_o^{s4} = 0$$

$$w_o^o = w_o^{c1} = w_o^{s1} = w_o^{c2} = w_o^{s2}$$

$$= \beta_\theta^o = \beta_\theta^{c1} = \beta_\theta^{s1} = \beta_\theta^{c2} = \beta_\theta^{s2} = 0 \qquad at\ x = 0, L.$$

Clamped-clamped:

$$u_o^o = u_o^{c1} = u_o^{s1} = u_o^{c2} = u_o^{s2} = u_o^{c3} = u_o^{s3} = u_o^{c4} = u_o^{s4}$$

$$= v_o^o = v_o^{c1} = v_o^{s1} = v_o^{c2} = v_o^{s2} = v_o^{c3} = v_o^{s3} = v_o^{c4} = v_o^{s4} = 0$$

$$w_o^o = w_o^{c1} = w_o^{s1} = w_o^{c2} = w_o^{s2} = \beta_s^o = \beta_s^{c1} = \beta_s^{s1} = \beta_s^{c2} = \beta_s^{s2}$$

$$= \beta_\theta^o = \beta_\theta^{c1} = \beta_\theta^{s1} = \beta_\theta^{c2} = \beta_\theta^{s2} = 0 \qquad at\ x = 0, L.$$

Based on progressive mesh refinement, 48 elements idealization is found to be adequate to model the complete slant length of the conical shells. The present formulation is validated considering thermal buckling of cross-ply circular cylindrical and conical shells for which solutions are available in the literature, and the results are presented in Table-1 and Table-2. It can be seen from these tables that the present results are in reasonably good agreement with the available solutions in the literature. Furthermore, the present results are in excellent agreement with those evaluated using ANSYS 8.0 software with 128 x 32 converged mesh discretization in the circumferential and meridional directions of the full shell employing Shell 99

Table-1 : Comparison of critical buckling temperature for cross-ply simply supported circular cylindrical shells ($L/r_1 = 0.5$, $r_1 = r_2$; Longitudinal wave number $m = 3$; $E_L/E_T = 10$, $G_{LT}/E_T = 0.5$, $G_{TT}/E_T = 0.5$, $\nu_{LT} = \nu_{TT} = 0.25$, $\alpha_T/\alpha_L = 2.0$, $\alpha_L = 1 \times 10^{-6}$/°C)

R_o/h	Critical Temperature (°C)					
	90°/0°			90°/0°/90°		
	Ref [4]	Present	ANSYS	Ref [4]	Present	ANSYS
200	1188.950 (13)*	1144.9921 (12)	1145.8877 (12)	1304.298 (11)	1199.8854 (11)	1201.2332 (11)
		1131.7327 (13)	1132.8047 (13)		1197.8608 (12)	1199.4305 (12)
		1137.7563 (14)	1139.0940 (14)		1234.2731 (13)	1236.2007 (13)
300	756.398 (15)	698.9543 (15)	699.9738 (15)	912.434 (13)	843.8837 (13)	844.8075 (13)
		696.0731 (16)	697.3430 (16)		843.1547 (14)	844.2207 (14)
		704.3311 (17)	705.9221 (17)		866.5438 (15)	867.7775 (15)
400	553.418 (18)	507.1465 (17)	508.6172 (17)	659.610 (18)	596.1045 (16)	597.3058 (16)
		504.8755 (18)	506.6338 (18)		594.0274 (17)	595.4641 (17)
		509.7994 (19)	511.9068 (19)		599.7064 (18)	601.4411 (18)
500	452.986 (19)	397.8804 (19)	399.8821 (19)	514.745 (19)	484.2163 (17)	485.6926 (17)
		397.2005 (20)	399.5241 (20)		478.6606 (18)	480.3878 (18)
		400.9850 (21)	403.6737 (21)		479.1408 (19)	481.1822 (19)

* *Numbers in bracket indicate circumferential wave number*

Table-2 : Comparison of critical buckling temperature parameter ($\lambda_T = 10^3\ \alpha_T\ \Delta T$) for cross-ply $(0°/90°)_{N/2}$ simply supported circular conical shells ($L/r_1 = 5.0$, $r_1/h = 10$)

ϕ	n	N	Ref [23]		Present*	Present	ANSYS
			3D solution	Classical solution			
30°	4	2	2.5364	2.8713	2.6825	12.8089	12.3342
	3	4	4.1262	4.7550	4.1452	16.4601	16.5283
	3	6	4.4064	5.0550	4.3299	17.4403	17.2816
45°	4	2	1.9520	2.1839	2.1476	9.4392	9.1151
	3	4	3.2862	3.7222	3.4224	12.1112	11.7051
	3	6	3.4750	3.9243	3.5409	12.8411	12.2130
60°	4	2	1.4514	1.6149	1.6234	6.3580	6.3229
	3	4	2.3719	2.6763	2.4965	8.3121	8.1648
	3	6	2.5045	2.8196	2.5825	8.8269	8.6797

** Initial prebuckling thermal stresses evaluated as in Ref.[23]*

(Eight noded linear layered structural shell) element. The comparison of thermal postbuckling behavior predicted based on the present formulation is made with Ref. [11] for cross-ply laminated cylindrical shells. The results are presented in Fig.1 as temperature parameter versus maximum asymmetric displacement $\left(w_o^{c1}/h\right)$ curve and are found to be reasonably close. The present formulation is also validated by comparing the critical bifurcation temperature value of 96.6578°F of evaluated from the present nonlinear analysis for a clamped-clamped conical shell fabricated from brass sheet (r_1/h = 366, L/r_1 = 2.83, h = 0.005 inch, $\alpha = 10.4 \times 10^{-6}/^0$F, $\phi = 15^0$) with the available theoretical result of 98°F reported in Ref. [20]. However, the experimental value of buckling temperature observed in Ref. [20] is 128°F. The discrepancy between the theoretical and experimental results is attributed to the determination of buckling by visual inspection as mentioned in [20]. To clarify this, the nonlinear thermoelastic response of the shell evaluated in the present study is depicted in Fig. 2. It can be observed from this figure that the shell shows snap-through type of postbuckling response and the maximum outward displacement at 128°F temperature is about three times the thickness of the shell whereas the

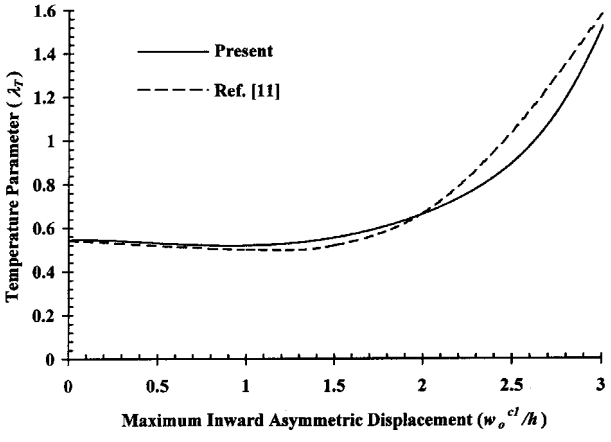

Fig.1 Comparison of thermal postbuckling curve for cross-ply $(0°/90°)_s$ laminated clamped-clamped cylindrical shell (L = 3m, r_1=r_2=3.8197m, h = 0.01 m; E_L = 130.3 GPa, E_T =9.377 GPa, G_{LT} = 4.502 GPa, ν_{LT} = 0.33, $\alpha_L = 0.139 \times 10^{-6}$, $\alpha_T = 9.0 \times 10^{-6}$; n = 14)

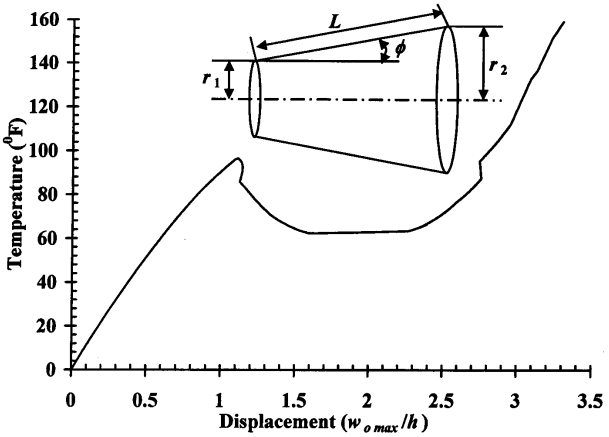

Fig.2 Temperature versus maximum displacement (w_{max}/h) curve for clamped-clamped isotropic circular conical shell (r_1/h =366,L/r_1 = 2.83, h = 0.005 in., $\alpha = 10.4 \times 10^{-6}/°F$, ϕ = 15°)

inward displacement (not shown in the figure) is about six times of the thickness. For the thin shell considered in experimental investigation [20], this amplitude level of deformation may be considered minimum deformation being visually observable.

Firstly, the distribution of prebuckling in-plane stress resultants (N_{ss}, $N_{\theta\theta}$, $N_{s\theta}$) ,whose compressive nature is responsible for thermoelastic buckling, along the meridional direction for two-layered angle-ply (θ/-θ) conical shells considering different values of ply-angle (θ = 15°, 45° and 75°) and semi-cone angle (ϕ = 0°, 30° and 60°) is depicted in Fig.3. It can be observed from this figure that the distribution of meridional and in-plane shear stress resultants (N_{ss}, $N_{s\theta}$) is uniform for cylindrical shells (ϕ = 0°, case) whereas for conical shells (ϕ = 30°, 60°) the distribution is nonlinear with decreasing trend in the magnitude from smaller diameter section to larger diameter section. In general, the magnitude of N_{ss} and $N_{s\theta}$ increases near the smaller section and decreases near the larger one with increase in the semi-cone angle (ϕ). The oscillations in the stresses near the supports/ends of the shells observed in this figure for some cases may be attributed to the boundary layer effects. It can further be noticed from this figure that the hoop stress resultant $N_{s\theta}$ is maximum near the support/end sections of the shells and vanishes away from supports. It can also be viewed from Fig.3 that the stress resultant N_{ss} decreases significantly for 45° and 75° ply-angle cases compared to shells with 15°/-15° lamination scheme and the minimum magnitude of N_{ss} being at 45° ply-angle. However, the magnitude of hoop resultant $N_{\theta\theta}$ increases with ply-angle and maximum is observed at 75° ply-angle. The magnitude of shear stress resultant ($N_{s\theta}$) is significantly lower compared to meridional and hoop components. The combined influence of N_{ss} and $N_{\theta\theta}$ leads to the onset of asymmetric ($n \neq 0$) thermoelastic buckling at lowest critical temperature for shells with 15° and 75° ply-angles and axisymmetric ($n = 0$) buckling/deformation for shells with 45° ply-angle as observed through linear eigenvalue analysis (results are not presented here for sake of brevity) and nonlinear static response analysis discussed subsequently.

Next, the nonlinear thermoelastic response characteristics of two-layered angle-ply laminated (15°/-15°) simply supported conical shells ($L/r_1 = 2$, $r_1/h = 100$) are shown in Fig.4 for different values of semi-cone angle (ϕ = 0°, 15°, 30°, 45°, 60°) and circumferential wave number (n = 8, 9). The circumferential wave numbers

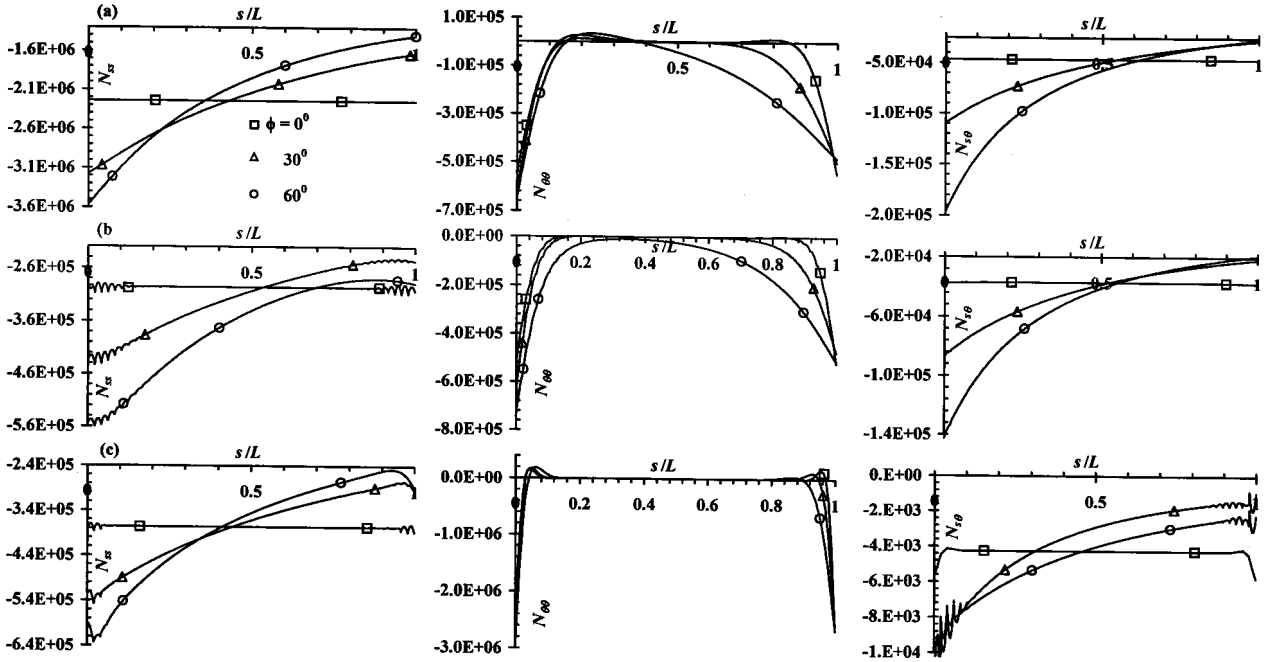

Fig.3 In-plane stress resultants (N_{ss}, $N_{\theta\theta}$, $N_{s\theta}$) distribution along the meridional direction for two-layered angle-ply shells ($L/r_1 = 2$, $r1/h = 100$) (a) 15°/-15°, (b) 45°/-45°, (c) 75°/-75°

chosen here correspond to the lowest bifurcation temperature. It can be observed from this figure that the transverse displacement increases with the temperature parameter up to a certain value beyond which the equilibrium path shows bifurcation buckling from purely axisymmetric deformation to combination of axisymmetric and asymmetric deformation. The prebuckling responses of the shells reveal softening type of nonlinear nature i.e. the rate

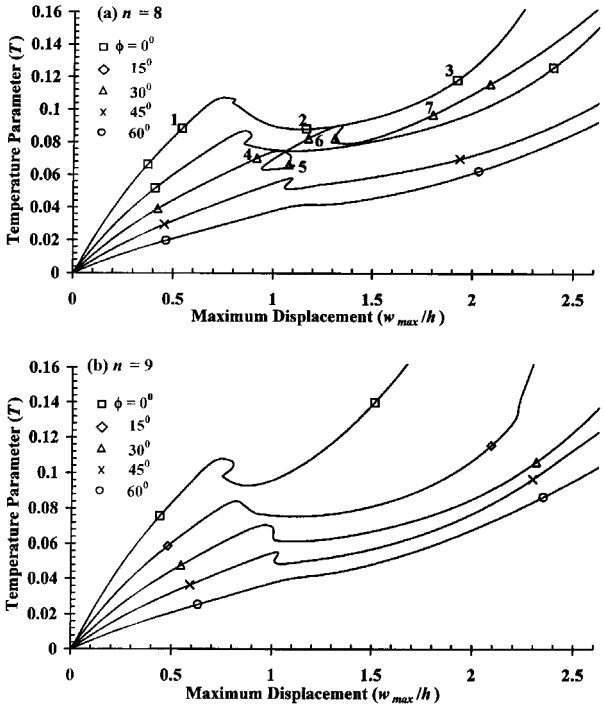

Fig.4 Nonlinear thermoelastic response curves for two-layered angle-ply laminated (15°/-15°) simply-supported conical shells ($L/r_1 = 2$, $r_1/h = 100$): (a) n=8, (b) n = 9

of increase of the prebuckling response shows increasing trend with the increase in temperature parameter. It can also be noticed from Fig. 4 that the critical bifurcation temperature decreases and the associated prebuckling deformation level increases with the increase in the semi-cone angle (ϕ). After the bifurcation point, the snap-through type of postbuckling response is predicted except for shallow conical shells ($\phi = 60°$). For the shallow conical shells, the postbuckling response is of stable nature i.e. the postbuckling strength/temperature increases with the increasing displacement. Furthermore, the postbuckling response shows hardening type of nonlinear nature away from the vicinity of bifurcation and the degree of hardening nonlinearity is decreased at higher values of the semi-cone angle. The difference in the temperature parameter corresponding to bifurcation point and minimum equilibrium temperature in the postbuckling path is, in general, decreasing with the semi-cone angle indicating that the sensitivity to imperfection decreases with the semi-cone angle. The variation of axisymmetric and asymmetric normal displacement components along the meridional direction is depicted in Fig.5 for cylindrical ($\phi = 0°$) and conical ($\phi = 30°$) shells corresponding to the points marked in Fig.4(a). It can be inferred from Fig.5 that the prebuckling response prior to the bifurcation point is dominated by axisymmetric component. The participation of asymmetric components is significantly lower in the prebuckling region whereas the postbuckling response is dominated by asymmetric components. It can further be inferred from Fig.5 that the relative contribution and meridional variation of axisymmetric/asymmetric displacement components changes significantly after the bifurcation point. This phenomenon is associated with the decreasing trend of temperature parameter and/or maximum displacement after the occurrence of the bifurcation or the formation of loops in the postbuckling equilibrium

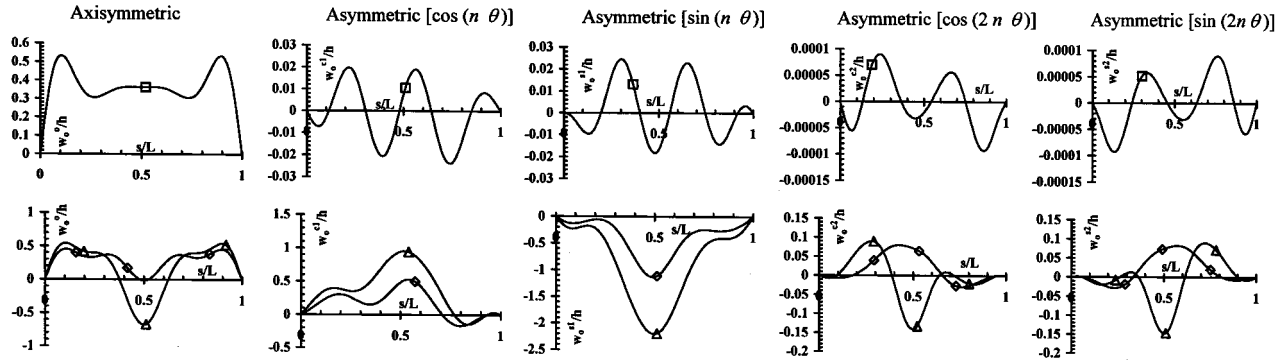

Fig.5(a) Variation of normal displacement components along the meridional direction for two-layered angle-ply shell ($L/r_1 = 2$, $r_1/h = 100$, $\phi = 0°$, 15°/-15°) □Point No. 1 [Fig.4(a)]; ◊Point No.2; Δ Point No.3

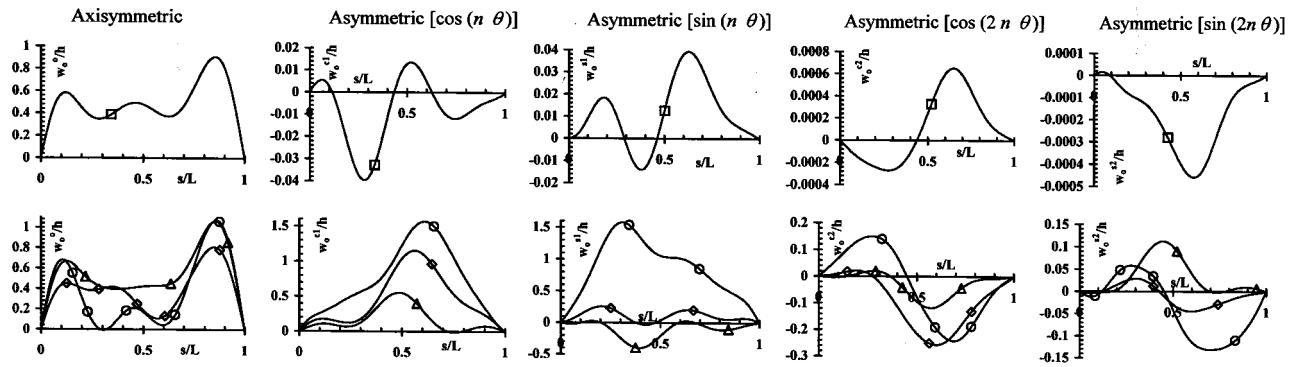

Fig.5(b) Variation of normal displacement components along the meridional direction for two-layered angle-ply shell ($L/r_1 = 2$, $r_1/h = 100$, $\phi = 30°$, 15°/-15°) □Point No. 4 [Fig.4(a)]; ◊ Point No.5; Δ Point No.6; o Point No.7

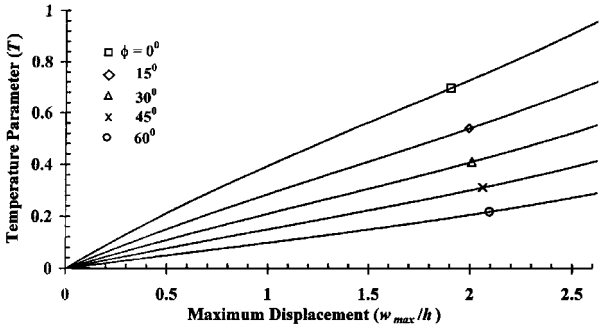

Fig.6 Nonlinear thermoelastic response curves for two-layered angle-ply laminated (45°/-45°) simply-supported conical shells ($L/r_1 = 2$, $r_1/h = 100$)

path, as observed in Fig.4. It may be noted here that the uniform rise in temperature leads to the outward axisymmetric transverse deformation of the shell due to circumferential thermal expansion unlike the perfect flat structures where the transverse displacement is zero until the critical/bifurcation point.

The nonlinear response behaviors of two-layered angle-ply laminated (θ/-θ) simply supported conical shells ($L/r_1 = 2$, $r_1/h = 100$) for ply angle $\theta = 45°$ and 75° cases are shown in Figs. 6 and 7, respectively. It can be noticed from Fig.6 that the shells with 45°/-45° lamination scheme do not exhibit asymmetric bifurcation buckling. However, it is revealed from Fig.7 that the shells with 75°/-75° lamination scheme exhibit bifurcation buckling at significantly higher temperature compared to shells with 15°/15° lamination scheme. Furthermore, the postbuckling characteristics of 75°/-75° laminated shells are even qualitatively different from those of 15°/-15° lamination scheme. The insight into the deformation pattern associated with

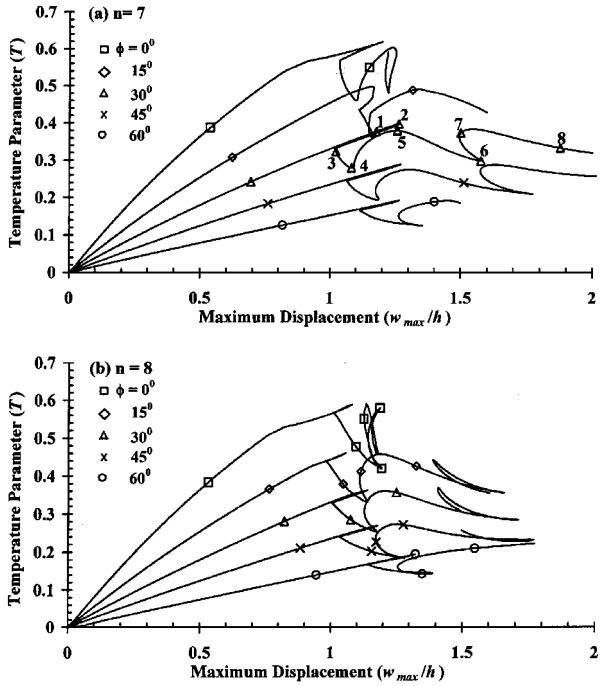

Fig.7 Nonlinear thermoelastic response curves for two-layered angle-ply laminated (75°/-75°) simply-supported conical shells ($L/r_1 = 2$, $r_1/h = 100$): (a) n=7, (b) n=8

the typical postbuckling characteristics of 75°/-75° laminated shells can be gained from the study of the participation of axisymmetric and asymmetric normal displacement components highlighted in Fig.8 corresponding to the different points marked in Fig.7(a) for the conical shell ($\phi = 30°$). It can be seen from Fig.8 that the participation of asymmetric displacement components increases along the equilibrium path segments (see Fig.7) 1-2-3-4, 5-6, and 7-8, and it decreases along segments 4-5 and 6-7. The axisymmetric displacement component

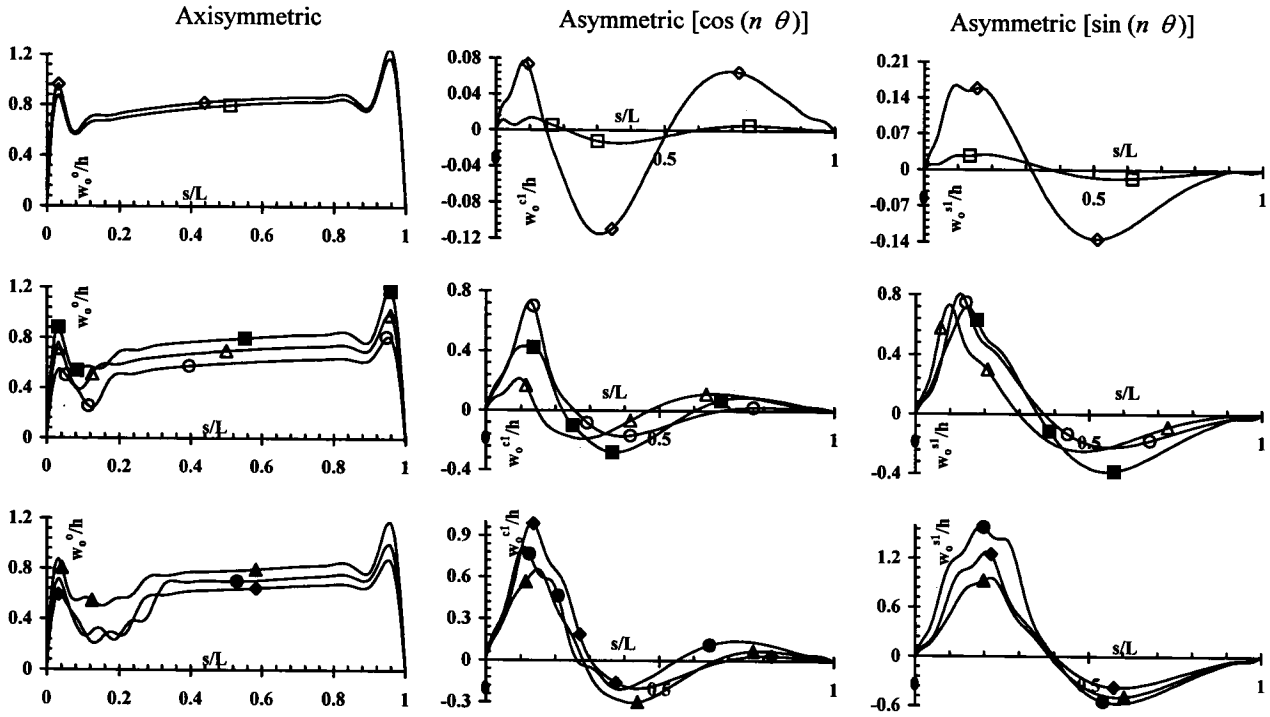

Fig.8 Variation of normal displacement components along the meridional direction for two-layered angle-ply shell ($L/r_1 = 2$, $r_1/h = 100$, $\phi = 30°$, 75°/-75°) □ Point No. 1 [Fig.7(a)]; ◊ Point No.2; Δ Point No.3; o Point No.4; ■ Point No.5; ◆ Point No.6; ▲ Point No.7; ● Point No.8

shows increasing trend along the postbuckling equilibrium path segments 4-5 and 6- 7, and decreasing one along segments 2-3-4, 5-6 and 7-8. Thus it can be interpreted that the decrease in the temperature along the postbuckling equilibrium path is associated with the increase in the asymmetric and decrease in the axisymmetric displacement components, and vice versa.

To highlight the influence of bending-stretching coupling due to lamination scheme, the nonlinear thermoelastic response of three-layered shells (15°/-15°/15°) is analyzed and depicted in Fig.9. It can be observed from Fig.9 that the pre- and postbuckling thermoelastic response characteristics of symmetrically laminated shells are qualitatively similar to those of two-layered shells. However, the critical bifurcation temperature, the difference in the temperature corresponding to bifurcation and minimum equilibrium postbuckling temperature, and the postbuckling strength/temperature are noticeably higher compared to two-layered shells.

Finally, the nonlinear pre- and post-buckling behavior of two-layered cross-ply (0°/90°) shells is studied and the results are shown in Fig.10. It can be viewed from this figure that the critical bifurcation temperature and the associated prebuckling deformation level are considerably lower compared to angle-ply shells. It can also be inferred from Fig.10 that the postbuckling response is of stable nature, and the postbuckling strength/degree of hardening nonlinearity in the postbuckling region is very low in comparison with angle-ply shells for all the semi-cone angles considered here. Furthermore, it is observed from the study of the buckling mode shapes of cross-ply shells (not presented here) that in the postbuckling analysis of cross- ply shells, only one pair of the asymmetric transverse displacement components, either w_o^{c1} and w_o^{c2} [corresponding to cos ($n\theta$) and cos (2 $n\theta$)] or w_o^{s1} and w_o^{s2} [corresponding to sin ($n\theta$) and sin (2 $n\theta$)] participate in the response in addition to axisymmetric one unlike the angle-ply shells requiring the incorporation of all asymmetric components w_o^{c1} , w_o^{s1} , w_o^{c2} and w_o^{s2}.

Conclusions

The nonlinear thermoelastic buckling/postbuckling characteristics of angle- and cross-ply laminated truncated circular conical shells subjected to uniform temperature rise are studied employing semi-analytical finite element approach. The participation of axisymmetric and asym-

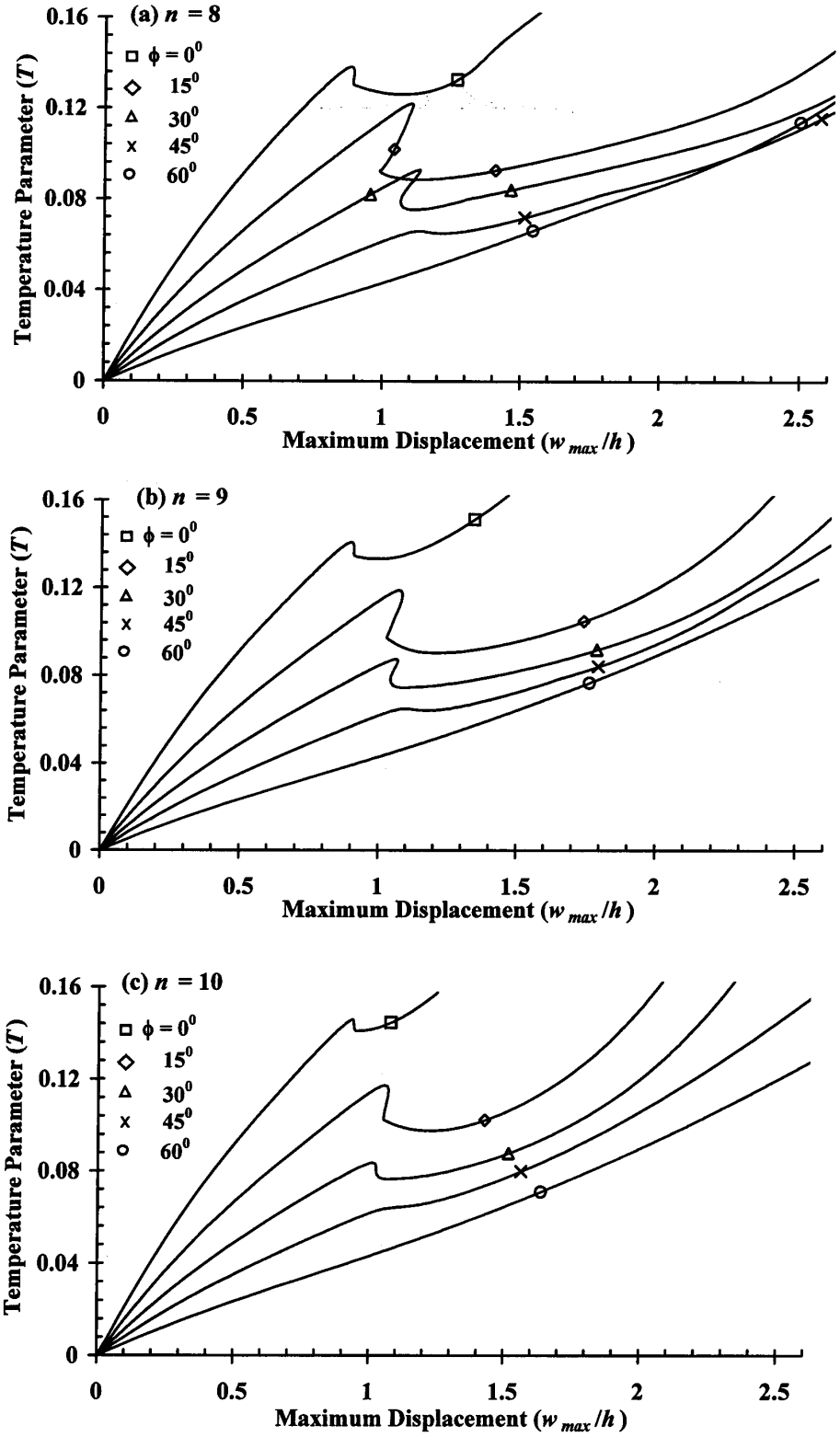

Fig.9 Nonlinear thermoelastic response curves for three-layered angle-ply laminated (15°/-15°/15°) simply-supported conical shells (L/r_1 = 2, r_1/h = 100) (a) n=8, (b) n=9, (c) n=10

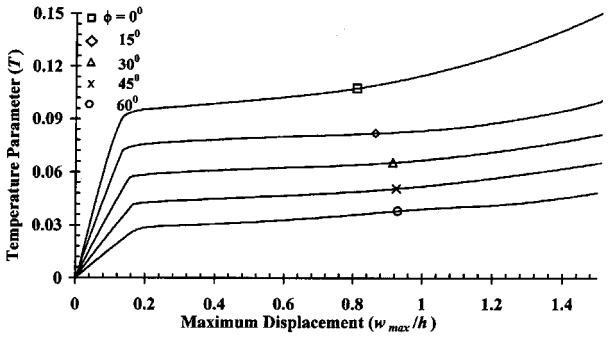

Fig.10 Nonlinear thermoelastic response curves for two-layered angle-ply laminated (0°/90°) simply-supported conical shells ($L/r_1 = 2$, $r_1/h = 100$; n=8)

metric modes in the total response of the shells is brought out through the deformation shape analysis. The following observations can be made from the detailed analysis carried out here:

a) The combined influence of meridional and hoop stress resultants leads to the onset of asymmetric thermoelastic buckling at lowest critical temperature for shells with 15° and 75° ply-angles and axisymmetric buckling/deformation for shells with 45° ply-angle.

b) The prebuckling responses of the shells reveal softening type of nonlinear nature.

c) The axisymmetric nature of the nonlinear thermoelastic response before the bifurcation of equilibrium path changes to combination of axisymmetric and asymmetric deformations after bifurcation.

d) The critical bifurcation temperature decreases and the associated prebuckling deformation level increases with the increase in the semi-cone angle.

e) The snap-through type of post buckling response is revealed for angle-ply (15°/-15°) shells with semi-cone angle ϕ = 0°, 15°, 30°, 45° and stable one for shallow conical shells (ϕ = 60°).

f) The postbuckling response shows hardening type of nonlinear nature away from the vicinity of bifurcation and the degree of hardening nonlinearity is decreased at higher values of the semi-cone angle.

g) The sensitivity to imperfection of angle-ply (15°/-15°) shells decreases with the semi-cone angle.

h) The changes in the relative contribution and meridional distribution of axisymmetric/asymmetric displacement components lead to the formation of loops in the postbuckling equilibrium path for certain shell parameters.

i) The shells with 45°/-45° lamination scheme do not exhibit asymmetric bifurcation buckling whereas 75°/-75° shells exhibit bifurcation buckling at significantly higher temperature compared to 15°/-15° lamination scheme.

j) The postbuckling characteristics of 75°/-75° laminated shells are significantly different from those of 15°/-15° lamination scheme.

k) The critical bifurcation temperature, the difference in the temperature corresponding to bifurcation and minimum equilibrium postbuckling temperature, and the postbuckling strength are noticeably higher for three layered shells (15°/-15°/15°) compared to two-layered shells (15°/-15°).

l) The postbuckling response of cross-ply shells is of stable nature and the postbuckling strength/degree of hardening nonlinearity is very low in comparison with angle-ply (15°/-15°) shells.

References

1. Thornton, E. A., "Thermal Buckling of Plates and shells", Applied Mechanics Reviews, Vol. 46, pp. 485- 506, 1993.

2. Noor, A. K. and Burton, W. S., "Computational Models for High-temperature Multilayered Composite Plates and Shells", Applied Mechanics Reviews, Vol. 45, pp. 419-446, 1992.

3. Argyris, J. H. and Tenek, L., "Recent Advances in Computational Thermostructural Analysis of Composite Plates and Shells with Strong Nonlinearities", Applied Mechanics Reviews, Vol. 50, pp. 285-305, 1997.

4. Thangartnam, R. K., Palaninathan, R. and Ramachandran, J., "Buckling of Composite Cylindrical Shells", Journal of the Aeronautical Society of India, Vol. 41, pp. 47-54, 1989.

5. Thangartnam, R. K., Palaninathan, R. and Ramachandran, J., "Thermal Buckling of Lamianted Composite Shells", AIAA Journal, Vol. 28, pp. 859-860, 1990.

6. Eslami, M. R. and Javaheri, M. R., "Thermal and Mechanical Buckling of Composite Cylindrical Shells", Journal of Thermal Stresses, Vol. 22, pp. 527-545, 1999.

7. Ganesan, N. and Kadoli, R., "Buckling and Dynamic Analysis of Piezothermoelastic Composite Cylindrical shells", Compos. Struct, Vol. 59, pp. 45-60, 2003.

8. Kadoli, R. and Ganesan, N., "Free Vibration and Buckling Analysis of Composite Cylindrical Shells Conveying Hot Fluid", Compos. Struct, Vol. 60, pp. 19-32,2003.

9. Birman, V. and Bert, C. W., "Buckling and Postbuckling of Composite Plates and Shells Subjected to Elevated Temperature", ASME J Appl Mech, Vol. 60, pp. 514-519, 1993.

10. Shen, H.-S., "Thermomechanical Postbuckling Analysis of Stiffened Laminated Cylindrical Shell", ASCE J Engineering Mechanics, Vol. 123, pp. 433-443, 1997.

11. Shen, H.-S., "Thermal Postbuckling Analysis of Imperfect Stiffened Laminated Cylindrical Shells", International Journal of Nonlinear Mechanics, Vol. 32, pp. 259-275, 1997.

12. Shen, H.-S., "Postbuckling Analysis of Imperfect Stiffened Laminated Cylindrical Shells Under Combined External Pressure and Thermal Loading", International Journal of Mechanical Sciences, Vol. 40, pp. 339-355, 1998.

13. Shen, H.-S., "Postbuckling of Laminated Cylindrical Shells with Piezoelectric Actuators Under Combined External Pressure and Heating", International Journal of Solids and Structures, Vol. 39, pp. 4271-4289, 2002.

14. Shen, H.-S., "Thermomechanical Postbuckling of Shear Deformable Laminated Cylindrical Shells with Local Geometric Imperfections", International Journal of Solids and Structures, Vol. 39, pp. 4525-4542, 2002.

15. Birman, V., "Thermal Dynamic Problems of Reinforced Composite Cylinders", ASME Journal of Applied Mechanics, Vol. 57, pp. 941-947, 1990.

16. Shariyat, M. and Eslami, M. R., "Dynamic Buckling and Postbuckling of Imperfect Orthotropic Cylindrical Shells Under Mechanical and Thermal Loads, Based on the Three-dimensional Theory of Elasticity", ASME Journal of Applied Mechanics, Vol. 66, pp. 476-484, 1999.

17. Birman, V. and Bert, C. W., "Dynamic Stability of Reinforced Composite Cylindrical Shells in Thermal Fields", Journal of Sound and Vibration, Vol. 142, pp. 183-190, 1990.

18. Bendavid, D. and Singer, J., "Buckling of Conical Shells Heated Along a Generator", AIAA Journal, Vol. 5, pp. 1710-1713,1967.

19. Lu, S. Y. and Chang, L. K., "Thermal Buckling of Conical Shells", AIAA Journal, Vol. 5, pp. 1877-1882, 1967.

20. Chang, L. K. and Lu, S. Y., "Nonlinear Thermal Elastic Buckling of Conical Shells", Nuclear Engineering and Design, Vol. 7, pp. 159-169, 1968.

21. Tani, J., "Influence of Axisymmetric Initial Deflections on the Thermal Buckling of Truncated Conical Shells", Nuclear Engineering and Design, Vol. 48, pp. 393-403, 1978.

22. Tani, J., "Buckling of Truncated Conical Shells Under Combined Pressure and Heating", Journal of Thermal Stresses, Vol. 7, pp. 307-316, 1984.

23. Wu, C.-P. and Chiu, S.-J., "Thermoelastic Buckling of Lamianted Composite Conical Shells", Journal of Thermal Stresses, Vol. 24, pp. 881-901, 2001.

24. Wu, C.-P. and Chiu, S.-J., "Thermally Induced Dynamic Instabilty of Laminated Composite Conical Shells", International Journal of Solids and Structures, Vol. 39, pp. 3001-3021, 2002.

25. Uda, T., "Nonlinear Free Vibrations of Conical Shells", Journal of Sound and Vibration, Vol. 64, pp. 85-95, 1979.

26. Tong, P. and Pian, T. H. H., "Postbuckling Analysis of Shells of Revolution by the Finite Element Method", Thin Shell Structures, Y. C. Fung and E. E. Sechler (Editors), Prentice-Hall Inc., Englewood Cliffs, New Jersey, pp. 435-452, 1974.

27. Amabili, M., Pellicano, F. and Paidoussis, M. P., "Non-linear Dynamics and Stability of Circular Cylindrical Shells Containing Flowing Fluid-Part II: Large Amplitude Vibrations Without Flow", Journal of Sound and Vibration, Vol. 228, pp. 1103-1124, 1999.

28. Patel, B. P., Ganapathi, M., Makhecha, D. P. and Shah, P., "Large Amplitude Free Flexural Vibration of Rings Using Finite Element Approach", International Journal of Non-Linear Mechanics, Vol. 37, pp. 911-921, 2003.

29. Kraus, H., "Thin Elastic Shells", John Wiley and Sons Inc., New York, 1976.

30. Jones, R. M., "Mechanics of Composite Materials", McGraw-Hill, New York, 1975.

31. Rajasekaran, S. and Murray, D. W., "Incremental Finite Element Matrices", ASCE Journal of the Structural Division, Vol. 99, pp. 2423-2438, 1973.

32. Batoz, J. L. and Dhatt, G., "Incremental Displacement in Nonlinear Analysis", International Journal for Numerical Methods in Engineering, Vol. 14, pp. 1262-1267,1979.

33. Bergan, P. G. and Clough, R. W., "Convergence Criteria for Iterative Process", AIAA Journal, Vol. 10, pp. 1107-1108, 1972.

34. Balakrishna, C. and Sarma, B. S., "Analysis of Axisymmetric Shells Subjected to Asymmetric Loads Using Field Consistent Shear Flexible Curved Element", Journal of the Aeronautical Society of India, Vol. 41, pp. 89- 95, 1989.

35. Prathap, G. and Ramesh Babu, C., "A Field-consistent Three-noded Quadratic Curved Axisymmetric Shell Element", International Journal for Numerical Methods in Engineering, Vol. 23, pp. 711-723, 1986.